

# Anharmonic parametric excitation in optical lattices

R. Jáuregui

*Instituto de Física, Universidad Nacional Autónoma de México, Apdo. Postal 20-364, México, 01000, D.F., México*

N. Poli, G. Roati, and G. Modugno

*INFN-European Laboratory for Nonlinear Spectroscopy (LENS), Università di Firenze, Largo E. Fermi 2, 50125 Firenze, Italy*  
(October 20, 2018)

We study both experimentally and theoretically the losses induced by parametric excitation in far-off-resonance optical lattices. The atoms confined in a 1D sinusoidal lattice present an excitation spectrum and dynamics substantially different from those expected for a harmonic potential. We develop a model based on the actual atomic Hamiltonian in the lattice and we introduce semiempirically a broadening of the width of lattice energy bands which can physically arise from inhomogeneities and fluctuations of the lattice, and also from atomic collisions. The position and strength of the parametric resonances and the evolution of the number of trapped atoms are satisfactorily described by our model.

32.80.Pj, 32.80.Lg

## I. INTRODUCTION

The phenomenon of parametric excitation of the motion of cold trapped atoms has recently been the subject of several theoretical and experimental investigations [1–3]. The excitation caused by resonant amplitude noise has been proposed as one of the major sources of heating in far-off-resonance optical traps (FORTs), where the heating due to spontaneous scattering forces is strongly reduced [4]. In particular, the effect of resonant excitation is expected to be particularly important in optical lattices, which usually provide a very strong confinement to the atoms, resulting in a large vibrational frequency and in a correspondingly large transfer of energy from the noise field to the atoms [1].

Nevertheless, parametric excitation is not only a source of heating, but it also represents a very useful tool to characterize the spring constant of a FORT or in general of a trap for cold particles, and to study the dynamics of the trapped gas. Indeed, the trap frequencies can be measured by intentionally exciting the trap vibrational modes with a small modulation of the amplitude of the trapping potential, which results in heating [5] or losses [2,6] for the trapped atoms when the modulation frequency is tuned to twice the oscillation frequency. This procedure usually yields frequencies that satisfactorily agree with calculated values, and are indeed expected to be accurate for the atoms at the bottom of the trapping potential. From the measured trap frequencies is then possible to estimate quantities such as the trap depth and the number and phase space densities of trapped atoms.

We note that this kind of measurement is particularly important in optical lattices, since the spatial resolution of standard imaging techniques is usually not enough to estimate the atomic density from a measurement of the volume of a single lattice site.

Recently, 1D lattices have proved to be the proper environment to study collisional processes in large and dense samples of cold atoms, using a trapping potential independent for the magnetic state of the atoms. In this systems, the parametric excitation of the energetic vibrational mode along the lattice provides an efficient way to investigate the cross-dimensional rethermalization dynamics mediated by elastic collisions [7,6].

Most theoretical studies of parametric excitation rely on a classical [8] or quantum [1] harmonic approximation of the confining potential. Under certain circumstances these expressions show quite good agreement with experimental results [3]. However, general features of the optical lattice could be lost in these approaches. For example, a sinusoidal potential exhibits an energy band structure and a spread of transition energies, while harmonic oscillators have just a discrete equidistant spectrum. Thus, we might expect that the excitation process may happen at several frequencies, and with a non-negligible bandwidth. Such anharmonic effects can be important whenever the atoms are occupying a relatively large fraction of the lattice energy levels. The purpose of this paper is to give a simple description of parametric excitation in a sinusoidal 1D lattice. In the next Section, we briefly discuss general features of the stationary states on such a lattice. Then, we summarize the harmonic description given in Ref. [1] and extend it to the anharmonic case. By a numerical evaluation of transition rates, we make a temporal description of parametric excitation which is compared with experimental results. We discuss about the relevance of broadening of the spectral lines to understand the excitation process in this kind of systems. Some conclusions are given in the last Section.

## II. STATIONARY STATES OF A SINUSOIDAL OPTICAL LATTICE.

The Hamiltonian for an atom in a red detuned FORT is

$$H = \frac{P^2}{2M} + V_{\text{eff}}(\vec{x}), \quad (2.1)$$

with

$$V_{\text{eff}}(\vec{x}) = -\frac{1}{4}\alpha|\mathcal{E}(\vec{x})|^2, \quad (2.2)$$

where  $\alpha$  is the effective atomic polarizations and  $\mathcal{E}(x)$  is the radiation field amplitude. For the axial motion in a sinusoidal 1D lattice we can take

$$H_{ax} = \frac{P_z^2}{2M} + V_0 \cos^2(kz) \quad (2.3)$$

$$= \frac{P_z^2}{2M} + \frac{V_0}{2}(1 + \cos(2kz)). \quad (2.4)$$

The corresponding stationary Schrödinger equation

$$-\frac{\hbar^2}{2M} \frac{d^2\Phi}{dz^2} + \frac{V_0}{2}(1 + \cos(2kz))\Phi = E\Phi \quad (2.5)$$

can be written in canonical Mathieu's form

$$\frac{d^2\Phi}{du^2} + (a - 2q \cos 2u)\Phi = 0 \quad (2.6)$$

with

$$a = (E - \frac{V_0}{2})\left(\frac{2M}{\hbar^2 k^2}\right) \quad 2q = \frac{V_0}{2}\left(\frac{2M}{\hbar^2 k^2}\right). \quad (2.7)$$

It is well known that there exists countably infinite sets of characteristic values  $\{a_r\}$  and  $\{b_r\}$  which respectively yield even and odd periodic solutions of Mathieu equation. These values also separate regions of stability. In particular, for  $q \geq 0$  the band structure of the sinusoidal lattice corresponds to energy eigenvalues between  $a_r$  and  $b_{r+1}$  [11]. The unstable regions are between  $b_r$  and  $a_r$ . For  $q \gg 1$ , there is an analytical expression for the band width [11]:

$$b_{r+1} - a_r \sim 2^{4r+5} \sqrt{2/\pi} q^{\frac{1}{2}r + \frac{3}{4}} e^{-4\sqrt{q}}/r!. \quad (2.8)$$

The quantities defined above can be expressed in terms of a frequency  $\omega_0$  defined in the harmonic approximation of the potential

$$\frac{1}{2}M\omega_0^2 = \frac{V_0}{2} \frac{(2k)^2}{2!}, \quad (2.9)$$

thus obtaining

$$a = (E - \frac{V_0}{2})\left(\frac{4V_0}{\hbar^2\omega_0^2}\right); \quad q = \left(\frac{V_0}{\hbar\omega_0}\right)^2. \quad (2.10)$$

Thus, the width of the  $r$ -band can be estimated using Eq. (2.8) whenever the condition  $(V_0/\hbar\omega_0)^2 \gg 1$  is satisfied. In the experiment we shall be working with a 1D optical lattice having  $V_0 \sim 10.5\hbar\omega_0$ . While the lowest band  $r = 0$  has a negligible width  $\sim 10^{-18}\hbar\omega_0$ , the band widths for highest lying levels  $r = 10, 11, 12,$  and  $13$  would respectively be  $0.0065, 0.1036, 1.52,$  and  $20.56$  in units of  $\hbar\omega_0$ .

In order to determine the energy spectrum, a variational calculation can be performed. We considered a harmonic oscillator basis set centered in a given site of the lattice, and with frequency  $\omega_0$ . The diagonalization of the Hamiltonian matrix associated to (2.4) using 40 basis functions gives the eigenvalues  $E_n < V_0$  shown in Table I for  $V_0 = 10.5\hbar\omega_0$ . According to the results of last paragraph, the eigenvalues 12 and 13 belong to the same band while the band width for lower levels is smaller than  $0.11\hbar\omega_0$

### III. PARAMETRIC EXCITATION

As already mentioned, parametric excitation of the trapped atoms consists in applying a small modulation to the intensity of the trapping light,

$$H = \frac{P^2}{2M} + V_{\text{eff}}[1 + \epsilon(t)]. \quad (3.1)$$

Within first order perturbation theory, this additional field induces transitions between the stationary states  $n$  and  $m$  with an averaged rate

$$R_{m \leftarrow n} = \frac{1}{T} \left| \frac{-i}{\hbar} \int_0^T dt T(m, n) \epsilon(t) e^{i\omega_{mn}t} \right|^2 \\ = \frac{\pi}{2\hbar^2} |T(m, n)|^2 S(\omega_{mn}); \quad \omega_{mn} = \frac{E_m - E_n}{\hbar} \quad (3.2)$$

where

$$T(m, n) = \langle m | V_{\text{eff}} | n \rangle \\ = E_n \delta_{nm} - \frac{1}{2M} \langle m | \hat{P}^2 | n \rangle \quad (3.3)$$

is the matrix element of the space part of the perturbation and

$$S(\omega) = \frac{2}{\pi} \int_0^T d\tau \cos \omega\tau \langle \epsilon(t)\epsilon(t+\tau) \rangle \quad (3.4)$$

is the one-sided power spectrum of the two-time correlation function associated to the excitation field amplitude.

If the confining potential is approximated by a harmonic well, the transition rates different from zero are

$$R_{n \leftarrow n} = \frac{\pi\omega_0^2}{16} S(0)(2n+1) \quad (3.5)$$

$$R_{n \pm 2 \leftarrow n} = \frac{\pi\omega_0^2}{16} S(2\omega_0)(n+1 \pm 1)(n \pm 1) \quad (3.6)$$

The latter equation was used in [1] to obtain a simple expression for the heating rate,

$$\langle \dot{E} \rangle = \frac{\pi}{2} \omega_0^2 S(2\omega_0) \langle E \rangle, \quad (3.7)$$

showing its exponential character. The dependence on  $2\omega_0$  is characteristic of the parametric nature of the excitation process. The fact that  $\hbar$  is not present is consistent with the applicability of Eq. (3.7) in the classical regime.

Classically, parametric harmonic oscillators exhibit resonances not just at  $2\omega_0$  but also at  $2\omega_0/n$  with  $n$  any natural number [8]. In fact, the resonances corresponding to  $n=2$ , *i.e.* at an excitation frequency  $\omega_0$ , have been observed in optical lattices [2,6]. A quantum description of parametric harmonic excitation also predicts resonances at the same frequencies via  $n$ -th order perturbation theory [10]. In particular, the presence of the resonance at  $\omega_0$  can be justified with the following argument. According to the standard procedure, the second order correction to the transition amplitude between states  $|n\rangle$  and  $|m\rangle$  is given by

$$R_{m\leftarrow n}^{(2)} = \langle n|\mathcal{U}^{(2)}(t_0, t)|m\rangle = \sum_k \left(\frac{-i}{\hbar}\right)^2 T(n, k)T(k, m) \int_{t_0}^t dt' e^{i\omega_{nk}t'} \epsilon(t') \int_{t_0}^t dt'' e^{i\omega_{km}t''} \epsilon(t'') \quad (3.8)$$

with  $\mathcal{U}^{(2)}(t_0, t)$  the second order correction to the evolution operator  $\mathcal{U}$ . Therefore, the transition may be described as a two step procedure  $|m\rangle \leftarrow |k\rangle \leftarrow |n\rangle$ . For harmonic parametric excitation the matrix element of the space part of the perturbation differs from zero just for transitions  $|n\rangle \leftarrow |n\rangle$  and  $|n\pm 2\rangle \leftarrow |n\rangle$ . Consider a transition in Eq. (3.8) involving a "first" step in which the state does not change  $|n\rangle \leftarrow |n\rangle$  and a "second" step for which  $|n\pm 2\rangle \leftarrow |n\rangle$ . Then resonance phenomena occur when the total energy of the two excitations,  $2\hbar\Omega$ , coincides with that of the second step transition, *i. e.* for an excitation frequency  $\Omega = \omega_0$ .

These ideas can be directly extended to anharmonic potentials: the corresponding transition probability rates  $R(n, m)$  would be determined by the transition matrix  $T(n, m)$ , by the transition frequencies  $\omega_{nm}$  and by the time dependence of the excitation  $\epsilon(t)$ . In general, anharmonic transition matrix elements  $T(n, m)$  will be different from zero for a wider set of pairs  $(n, m)$ . Besides, the transition energies will not be unique so that the excitation process is *not* determined by the excitation power spectrum at a single given frequency  $2\omega_0$  and its subharmonics  $2\omega_0/n$ . As an example the transition energies for the specific potential considered in this work are reported in Table I. Therefore, within the model Hamiltonian of Eq. (3.1), resonance effects can occur for several frequencies that may alter the shape of the population distribution within the trap. However, in general these resonant excitations will not be associated with the escape of trapped atoms.

Here we are interested in a 1D lattice; the direct extension of the formalism mentioned above requires the evaluation of the matrix elements  $T(n, m)$  among the different Mathieu states that conform a band. This involves integrals which, to our knowledge, lack an analytical expression and require numerical evaluation. As an alternative, we consider functions which variationally approximate the Mathieu functions. They are the eigenstates of the Hamiltonian (2.4) in a harmonic basis set of frequency  $\omega_0$ :

$$|n\rangle = \sum_{i=1}^{i_{max}} c_{ni} |i\rangle_{\omega_0}, \quad (3.9)$$

These states are ordered according to their energy:  $E_n \leq E_{n+1}$  as exemplified in Table I. Within this scheme one obtains a very simple expression for  $T(n, m)$

$$T(n, m) = E_n \delta_{nm} - \sum_{i,j=1}^{i_{max}} c_{ni} c_{nj} \frac{1}{2M} \langle i|\hat{P}^2|j\rangle. \quad (3.10)$$

It is recognized that any discrete basis set approximation to a system with a band spectrum will lack features of the original problem which have to be carefully analyzed. Anyway, alternatives to a discrete basis approach may be cumbersome and not necessarily yield a better approach to understand general properties of experimental data. While the discrete basis approach is exact for transitions between the lowest levels, which have a negligible width, eigenstates belonging to a band of measurable width should be treated with special care. Thus, we shall assume that matrix elements  $T(\nu, \mu)$  involving states with energies  $\mathcal{E}_\nu$  and  $\mathcal{E}_\mu$ , so that  $E_n - (E_n - E_{n-1})/2 \leq \mathcal{E}_\nu \leq E_n + (E_{n+1} - E_n)/2$  with an analogous expressions for  $\mathcal{E}_\mu$ , are well approximated by  $T(n, m)$ .

Within this scheme the equations which describe the probability  $P(n)$  of finding an atom in level  $n$ , given the transition rates  $R_{m\leftarrow n}$  are

$$\dot{P}(n) = \sum_m R_{m\leftarrow n}^{(1)} (P(m) - P(n)) \quad (3.11)$$

in the first order perturbation theory scheme, and the finite difference equations

$$P_n(t) = P_n(t_0) + \sum_m R_{m\leftarrow n}^{(1)} (P_m(t_0) - P_n(t_0))(t - t_0) + \sum_m R_{m\leftarrow n}^{(2)} (P_m(t_0) - P_n(t_0))(t - t_0)^2, \quad (3.12)$$

valid up to second order time-dependent perturbation theory whenever  $t \sim t_0$ . Both sets of equations are subjected to the condition

$$\sum_n P(n) = 1. \quad (3.13)$$

Now, according to Eqs. (3.2) and Eq (3.8), the evaluation of  $R_{n\leftarrow m}^{(r)}$  also requires the specification of the spectral density  $S(\omega)$ . In the problem under consideration, the discrete labels  $m, n$  are used to calculate interband transitions which are actually spectrally broad. This broadening might arise not only from the band structure of the energy spectra associated with the Hamiltonian Eq. (2.4), but also from other sources, which we will discuss below. Broad spectral lines can be introduced in our

formalism by defining an effective spectral density  $S_{\text{eff}}(\omega)$  which should incorporate essential features of this broadening without simulating specific features. Having this in mind, an effective Gaussian density of states  $\mathcal{S}_n(\omega)$  is associated to each level  $|n\rangle$  of energy  $E_n$

$$\mathcal{S}_n(\omega) = \frac{1}{\sqrt{2\pi}\sigma_n} e^{-\frac{(\hbar\omega - E_n)^2}{2(\hbar\sigma_n)^2}}. \quad (3.14)$$

The spectral effective density  $S_{\text{eff}}(\omega_{nm})$  associated to the transition  $m \leftarrow n$  is obtained by the convolution of  $\mathcal{S}_n(\omega)$  with  $\mathcal{S}_m(\omega)$  and with the excitation source spectral density  $S(\omega)$ . For a monochromatic source the latter is also taken as a Gaussian centered at the modulation frequency that once integrated over all frequencies yields the square of the intensity of the modulation source. The net result is that  $S_{\text{eff}}(\omega_{nm})$  has the form

$$S_{\text{eff}}(\omega) = S_0 e^{-\frac{(\omega - \omega_{\text{eff}})^2}{2\sigma_{\text{eff}}^2}} \quad (3.15)$$

with  $\omega_{\text{eff}}$  determined by the modulation frequency  $\Omega$  and the energies  $E_n$  and  $E_m$ . The effective width  $\sigma_{\text{eff}}$  contains information about the frequency widths of the excitation source and those of each level.

#### IV. COMPARISON WITH EXPERIMENTAL RESULTS.

We have tested the procedure described in last section to model parametric excitation in a specific experiment conducted at LENS. In this experiment  $^{40}\text{K}$  fermionic atoms are trapped in a 1D lattice, realized retroreflecting linearly polarized light obtained from a single-mode Ti:Sa laser at  $\lambda=787\text{nm}$ , detuned on the red of both the  $D_1$  and  $D_2$  transition of potassium, respectively at  $769.9\text{nm}$ , and  $766.7\text{nm}$ . The laser radiation propagates along the vertical direction, to provide a strong confinement against gravity. The laser beam is weakly focused within a two-lens telescope to a waist size  $w_0 \simeq 90\ \mu\text{m}$ , with a Rayleigh length  $z_R=3\text{cm}$ ; the effective running power at the waist position is  $P=350\text{mW}$ .

The trap is loaded from a magneto-optical trap (MOT), thanks to a compression procedure already described in [6], with about  $5 \times 10^5$  atoms at a density around  $10^{11}\text{cm}^{-3}$ . The typical vertical extension of the trapped atomic cloud, as detected with a CCD camera (see Fig. 1), is  $500\ \mu\text{m}$ , corresponding to about 1200 occupied lattice sites with an average of 400 atoms in each site. Since the axial extension of the atomic cloud is much smaller than  $z_R$ , we can approximate the trap potential to

$$V(r, z) = V_0 e^{-\frac{2r^2}{w_0^2}} \cos^2(kz); \quad k = 2\pi/\lambda, \quad (4.1)$$

thus neglecting a 5% variation of  $V_0$  along the lattice. The atomic temperature in the lattice direction is measured with a time-of-flight technique and it is about  $50\ \mu\text{K}$ .

In order to parametrically excite the atoms we modulate the intensity of the confining laser with a fast AOM for a time interval  $T \simeq 100\text{ms}$ , with a sine of amplitude  $\epsilon=3\%$  and frequency  $\Omega$ . The variation of the number of trapped atoms is measured by illuminating the atoms with the MOT beams and collecting the resulting fluorescence on a photomultiplier. In Fig.2 the fraction of atoms left in the trap after the parametric excitation is reported *vs* the modulation frequency  $\Omega/2\pi$ . Three resonances in the trap losses are clearly seen at modulation frequencies  $340\text{kHz}$ ,  $670\text{kHz}$  and  $1280\text{kHz}$ . By identifying the first two resonances with the lattice vibrational frequency and its first harmonic, respectively, we get as first estimate  $\omega_0 \simeq 2\pi \times 340\text{kHz}$ . As we will show in the following, these resonance are actually on the *red* of  $\omega_0$  and  $2\omega_0$ , respectively, and therefore a better estimate is  $\omega_0 \simeq 2\pi \times 360\text{kHz}$ . Therefore the effective trap depth is, from Eq. (9),  $V_0 \simeq 185\ \mu\text{K} \simeq 10.5\ \hbar\omega_0$ . Since the atomic temperature is about  $V_0/3.5$ , we expect that most of the energy levels of the lattice have a nonnegligible population and therefore the anharmonicity of the potential could play an important role in the dynamics of parametric excitation. Note that the third resonance at high frequency, close to  $4\omega_0$ , is not predicted from the harmonic theory. It is possible to observe also a much weaker resonance in the trap losses around  $1.5\text{kHz}$ , which we interpret to be twice the oscillation frequency in the loosely confined radial direction. Anyway, in the following we will focus our attention just on the axial resonances.

As discussed in the previous Section, the overall width of the excitation assumed for our model system could play an important role in reproducing essential features of experimental data. Since the source used in the experiment has a negligible line width, it is necessary to model just the broadening of the atomic resonances. The spread of the transition energies due to the axial anharmonicity is reported in Table I, while the broadening of each energy level, due to the periodic character of the sine potential, is estimated using Eq. (2.8). We now note that the 1D motion assumed in Section II is not completely valid in our case, since the atoms move radially along a Gaussian potential. Since the period of the radial motion is about 500 times longer than the axial period, the atoms see an effective axial frequency which varies with their radial position, resulting in a broadening of the transition frequency. Other sources of broadening are fluctuations of the laser intensity and pointing, and inhomogeneities along the lattice. We note that also elastic collisions within the trapped sample, which tend to keep a thermal distribution of the trap levels population, can contribute to an overall broadening of the loss resonances. Since it is not easy to build a model which involve all these sources, we introduce semiempirically an effective broadening for the  $r$ -th level (see Eq. (3.14)).

Recognizing that the width could be energy dependent we considered the simple expression

$$\sigma_r^2 = \lambda_1 \left( \frac{E_r}{V_0} \right)^p + \lambda_0 \quad (4.2)$$

for several values of the constants  $\lambda_1, \lambda_0$  and  $p$ . When  $p = 0$ , i.e. for a constant value of the band width we were not able to reproduce the general experimental behavior reported in Fig.2. The best agreement between the simulation and the experimental observations is obtained for  $\lambda_0 = 0.0002$ ,  $\lambda_1 = 0.0135$ , in units of  $\omega_0^2$ , and  $p = 3$ . Similar results are obtained also for slightly higher (lower) values of  $\lambda_{0,1}$  together with slightly higher (lower) values of the power  $p$ . In Table I the resulting widths are shown for the lower twelve levels. Note that we have intentionally excluded levels 11, 12 and 13 from the calculation, since their intrinsic width is so large that the atoms can tunnel out of the trap along the lattice in much less than 100 ms [9]. Anyway, the inclusion of these levels proved not to change substantially the result of the simulation.

The comparison of experimental and theoretical results is made in Fig. 3; the abscissa for the experimental data has been normalized by identifying  $\omega_0$  with  $2\pi \times 360$  kHz. As already anticipated, the principal resonance in trap losses appears at  $\Omega \simeq 1.85\omega_0$ . This result follows from the fact that the excitation of the lowest trap levels is not resulting in a loss of atoms, as it would happen for a harmonic potential. On the contrary, the most energetic atoms, which have a vibrational frequency smaller than the harmonic one, are easily excited out of the trap. The asymmetry of the resonances, which has been observed also in [2], is well reproduced in the calculations and it is a further evidence of the spread of the vibrational frequencies. The first interesting result obtained by our study of parametric excitation is therefore the correction necessary to extract the actual harmonic frequency from the loss spectrum. For the specific conditions of the present experiment, we find indeed that the principal resonance in the trap losses appears at  $\Omega \simeq 1.85\omega_0$ . Anyway, the calculation shows that the resonance is nearby this position for all the explored values of  $\lambda_{0,1}$  and  $p$  also for deeper traps, up to  $V_0=25\hbar\omega_0$ , and therefore it appears to be an invariant characteristic of the sinusoidal potential.

The result of the numerical integration of Eqs. (3.12) reported in Fig.3 reproduces relatively well the subharmonic resonance, which in the harmonic case would be expected at  $\omega_0$ . On the contrary, both experiment and calculation show that the actual position of the resonance is  $\Omega \simeq 0.9\omega_0$ . It must be mentioned that the accuracy of these results is restricted by the finite difference character of Eqs. (3.12) and by the fact that some noise sources which have not been included could be resonant at a nearby frequency. In particular, a possible modulation of the laser pointing associated to the intensity modulation is expected to be resonant at  $\Omega = \omega_0$  in the harmonic

problem [1], and it could play an analogous role in our sinusoidal lattice.

The higher order resonance around  $3.5\omega_0$  observed in the experiment is also well reproduced by the calculations based on first order perturbation theory. Note that a simpler approximation to the confining potential by a quartic potential  $V_Q(z) = k_2 z^2 + k_4 z^4$  would yield a resonance around  $4\omega_0$  and not  $3.5\omega_0$ . Anyway, it is possible to understand qualitatively one of the features of this resonance considering a quartic perturbation of the form  $\epsilon(t)V_Q$  to a harmonic potential. In this case the ratio of the transition rates at the  $2\omega_0$  and  $4\omega_0$  resonances is set by Eqs.3.2 to

$$|T(n \pm 2, n)|^2 / |T(n \pm 4, n)|^2 \propto \frac{V_0^2}{\omega_0^2}. \quad (4.3)$$

This result can qualitatively explain the absence of the corresponding high order resonance in the *radial* excitation spectrum (see Fig.2): since the radial trap frequency is a factor 500 smaller than the axial one, the relative strength of such radial anharmonic resonance is expected to be suppressed by a factor  $(500)^2$ . In conclusion, high harmonics resonances, which certainly depend on the actual shape of the anharmonic potential, are expected to appear only if the spring constant of the trap is large.

In Fig.4 theoretical and experimental results for the evolution of the total population of trapped atoms at the resonant exciting frequency  $\Omega = 2\omega_0$  are shown. Although there is a satisfactory agreement between the model and the experiment, we notice that experimental data exhibit a different rate for the loss of atoms before and after 100 ms. This change is probably due to a variation of the collision rate as the number of trapped atoms is modified, which cannot be easily included in the model. The comparison of the experimental evolution of the trap population with and without modulation shows the effectiveness of the excitation process in emptying the trap on a short time-scale.

We have also simulated the energy growth of the trapped atoms due to the parametric excitation, which is reported in Fig. 5. Our calculations show nonexponential energy increase in contrast with what expected in the harmonic approximation, Eq. (3.7). The fast energy growth at short times is related to the depopulation of the lowest levels, which are resonant with the  $2\omega_0$  parametric source. The saturation effect observed for longer times is due to the fact that the resonance condition is not satisfied for the upper levels so that they do not depopulate easily.

## V. CONCLUSIONS.

We have studied both theoretically and experimentally the time evolution of the population of atoms trapped in a 1D sinusoidal optical lattice, following a parametric excitation of the lattice vibrational mode. In detail, we

have presented a theoretical model for the excitation in an anharmonic potential, which represents an extension of the previous harmonic models, and we have applied it to the actual sinusoidal potential used to trap cold potassium atoms. The simulation seems to reproduce relatively well the main features of both the spectrum of trap losses, including the appearance of resonances beyond  $2\omega_0$ , and the time evolution of the total number of trapped atoms.

By comparing the theoretical predictions and the experimental observations the usefulness of a parametric excitation procedure to characterize the spring constant of the trap has been verified. Although the loss resonances are red-shifted and wider than what expected in the harmonic case, the lattice harmonic frequency can be easily extracted from the experimental spectra, to estimate useful quantities such as the trap depth and spring constant.

We have also made emphasis on the need of modeling the broadening of bands with a negligible natural width in order to reproduce the observed loss spectrum. In a harmonic model this broadening is not necessary since the equidistant energy spectrum guarantees that a single transition energy characterizes the excitation process. We think that most of the broadening in our specific experiment is due to the fact that the actual trapping potential is not one-dimensional, and also to possible fluctuations and inhomogeneities of the lattice.

To conclude, we note that the dynamical analysis we have made can be easily extended to lattices with larger dimensionality, and also to other potentials, such as Gaussian potentials, which are also commonly used for optical trapping.

We acknowledge illuminating discussions with R. Brecha. This work was supported by the European Community Council (ECC) under the Contracts HPRI-CT-1999-00111 and HPRN-CT-2000-00125, and by MURST under the PRIN 1999 and PRIN 2000 Programs.

*Rev. Lett.* **82**, 1406 (1999).

- [8] L. D. Landau and E. M. Lifshitz, *Mechanics* (Pergamon, Oxford, 1976).
- [9] We estimate the mean velocity of the atoms along the lattice from the energy width of the levels as  $\bar{v} = \Delta\omega/2k$ .
- [10] R. Jáuregui, submitted for publication.
- [11] *Handbook of Mathematical Functions*, edited by M. Abramowitz and I. A. Stegun (Dover Publications, New York, 1965).

$r$	$E_r$	$E_{r+1} - E_r$	$\sigma_r$
0	0.494	0.976	0.014
1	1.470	0.95	0.015
2	2.420	0.923	0.019
3	3.343	0.897	0.025
4	4.240	0.867	0.032
5	5.107	0.837	0.042
6	5.944	0.802	0.051
7	6.746	0.767	0.062
8	7.513	0.727	0.072
9	8.240	0.680	0.082
10	8.920	0.624	0.092
11	9.544	0.551	–
12	10.095	0.402	–
13	10.497	–	–

TABLE I. Energy spectrum in units of  $\hbar\omega_0$  obtained from the diagonalization of the Hamiltonian Eq. (2.4) for  $V_0=10.5\hbar\omega_0$  in a harmonic basis set with the lowest 40 functions. The third column shows the band widths  $\sigma_r$ , Eqs. (3.14) and (4.2), used in the numerical simulations reported in Section IV.

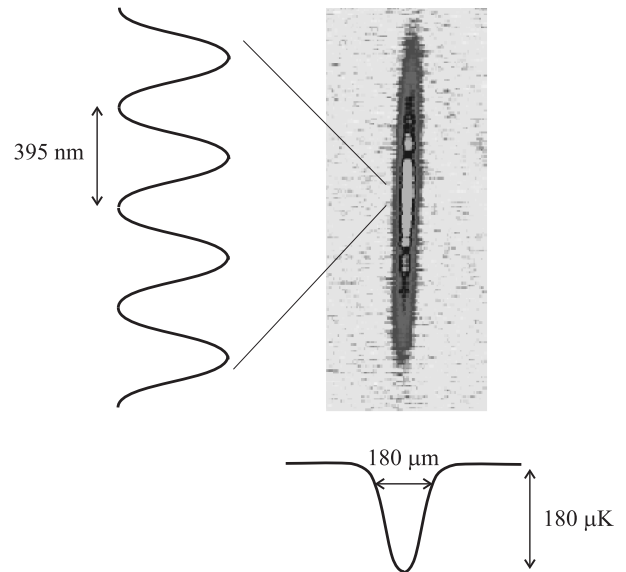


FIG. 1. Absorption image of the atoms in the optical lattice, and shape of the optical potential in the two relevant directions.

- [1] T. A. Savard, K. M. O'Hara, and J. E. Thomas, *Phys. Rev. A* **56**, R1095 (1997).
- [2] S. Friebe, C. D'Andrea, J. Walz, M. Weitz, and T. W. Hänsch, *Phys. Rev. A* **57**, R20 (1998).
- [3] C. W. Gardiner, J. Ye, H. C. Nagerl, and H. J. Kimble, *Phys. Rev. A* **61**, 045801 (2000).
- [4] J. D. Miller, R. A. Cline, and D. J. Heinzen, *Phys. Rev. A* **47**, R4567 (1993).
- [5] V. Vuletic, C. Chin, A. J. Kerman, and S. Chu, *Phys. Rev. Lett.* **81**, 5768 (1998).
- [6] G. Roati, W. Jastrzebski, A. Simoni, G. Modugno, and M. Inguscio, to appear in *Phys. Rev. A*; e-print: arXiv physics/0010065.
- [7] V. Vuletic, A. J. Kerman, C. Chin, and S. Chu, *Phys.*

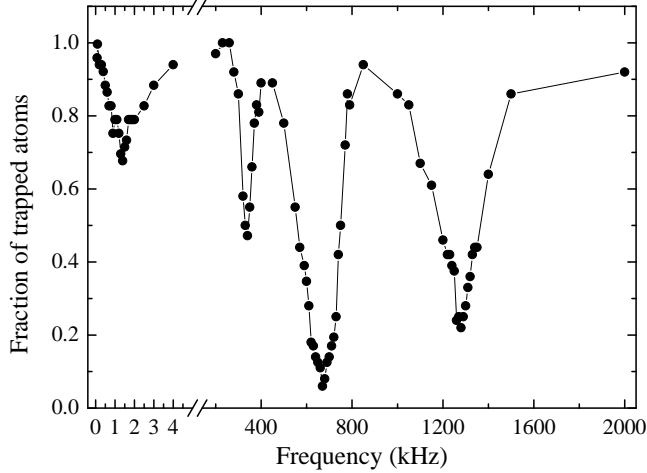


FIG. 2. Experimental spectrum of the losses associated to parametric excitation of the trap vibrational modes. For the low and high frequency regions two different modulation amplitudes of 20% and 3% respectively, were used.

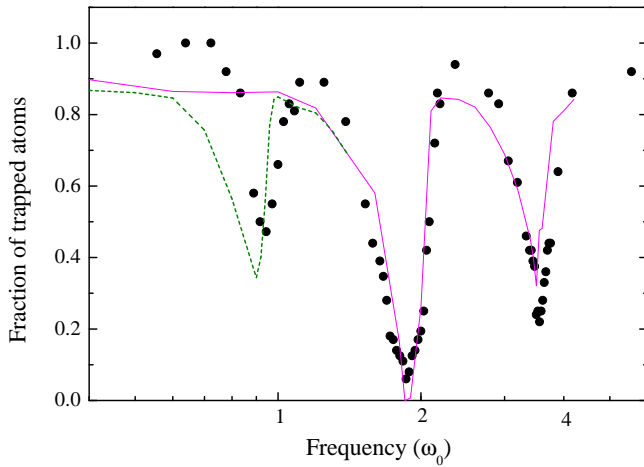


FIG. 3. Experimental (circles) and theoretical (lines) fraction of atoms left in the trap after parametric excitation *vs* the modulation frequency. The continuous line corresponds to the numerical integration of the first order perturbation theory equations (3.11) and the dashed line to the numerical integration of the finite difference second order perturbation theory equations (3.8).

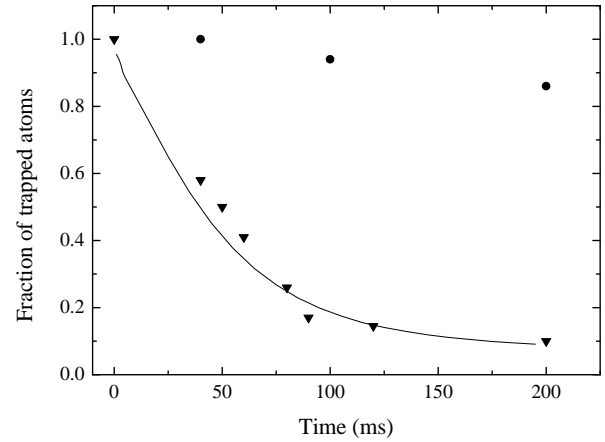


FIG. 4. Theoretical (continuous line) and experimental (triangles) results for the evolution of the population of trapped atoms at the resonant exciting frequency  $\Omega = 2\omega_0$ . The circles show the evolution of the population in absence of modulation.

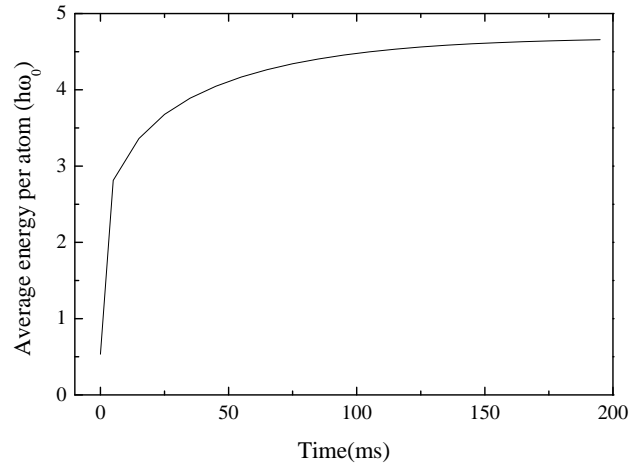


FIG. 5. Calculated evolution of the average energy of the trapped atoms during parametric excitation at  $\Omega = 2\omega_0$ .